# Effect of tip speed ratio on power coefficient of double savonius hydrokinetic water turbines

*Priyo* Heru Adiwibowo[1,2*], *Triyogi* Yuwono[1], *Wawan* Aries Widodo[1]

[1]Department of Mechanical Engineering, Faculty of Industrial Technology and Systems Engineering, Institut Teknologi Sepuluh Nopember, Kampus ITS Keputih Sukolilo, Surabaya 60111, Indonesia
[2]Department of Mechanical Engineering, Faculty of Engineering, Universitas Negeri Surabaya, Kampus Unesa 1, Jalan Kampus Unesa Ketintang, Surabaya 60231, Indonesia

**Abstract.** The growing global emphasis on sustainable development has increased demand for renewable energy sources. Hydrokinetic turbines have emerged as efficient and environmentally sustainable solutions for power generation in flowing water. The Savonius turbine is notable for its simple design, low maintenance requirements, and effective performance at low water velocities. This study examines the influence of Tip Speed Ratio (TSR) on the performance of a Savonius hydrokinetic turbine to identify optimal operating conditions. Numerical simulations were used to evaluate flow characteristics and performance metrics across a range of TSR values. The findings indicate that the power coefficient (Cp) attains its maximum at TSR = 1.0, corresponding to the highest energy conversion efficiency. Flow-contour analysis shows stable, symmetrical velocity and pressure distributions at this TSR, with well-formed vortices that produce maximum torque. The moment coefficient (Cm) decreases as TSR increases, reaching its highest value at low TSR (0.4–0.5). Therefore, TSR = 1.0 is determined to be the optimal operating point, balancing turbine efficiency and flow behavior, and offering practical guidance for the optimization of small-scale hydrokinetic energy systems.

## 1 Introduction

Using innovative, renewable energy sources is a key component of the global effort to address climate change and global warming. Accessibility for all societal groups must be given top priority in this program, with an emphasis on increasing access in developing countries [1], [2], [3]. The hydrokinetic turbine, currently under development, is a fascinating field of study in renewable energy technology. This hydrokinetic turbine's ability to capture and harness water's kinetic energy shows great potential and ingenuity.

This turbine has several advantages, including easy, affordable maintenance and the ability to be deployed across a range of water conditions. As previously said, the advantages make hydrokinetic turbines the best choice for producing environmentally friendly and sustainable energy [4], [5], [6], [7]. Large- and small-scale hydropower technologies are the two methods used to generate hydropower. By building dams or reservoirs, which alter hydraulic pressure, the potential energy of water is frequently captured for large-scale technology [8]. One characteristic of hydrokinetic technology is its small-scale approach. Through the motion of turbines, this technology captures the kinetic energy of the water and transforms it into mechanical work. The kinetic energy is then converted into electrical energy and distributed to the community [9].

From a physical standpoint, hydrokinetic turbines operate according to fluid-dynamic principles, in which the momentum of the flowing fluid exerts forces on the turbine blades. These forces generate torque and rotational motion, which can be characterized through parameters such as the Tip Speed Ratio (TSR), power coefficient (Cp), and moment coefficient (Cm). The TSR, defined as the ratio between the tangential blade tip speed and the incoming water velocity, directly influences the balance between drag and torque generation [10]. Determining the optimal TSR is essential to maximize power extraction efficiency [11].

Energy harvesting from low-rate water flow is most effectively achieved with Savonius-type turbines. These turbines have significant potential for development to enhance overall efficiency. Ongoing research efforts focus on innovation and advancement across design, optimization, and geometry. Numerous studies have been conducted on hydrokinetic turbines, including the work of Kumar et al. [12], who examined the blade design of the Savonius hydrokinetic turbine for sustainable energy applications. Rengma [13] assessed the turbine parameters influencing performance, while Doso and Gao [14] analyzed the Savonius rotor's power generation capabilities. In 2020, Nauman et

* Corresponding author: priyoheruadiwibowo@unesa.ac.id

al. [15] focused on optimizing and applying Savonius turbines. More recently, Moniruzzaman et al. [16] explored the future of hydrokinetic technology in Bangladesh, and Muhyiddin et al. [17] conducted a 2024 review that employed a specialized vertical-axis computational fluid dynamics (CFD) approach to analyze hydrokinetic turbines.

The Savonius turbine offers advantages such as self-starting ability and straightforward design. Its rotor is formed like an S and usually has concave and convex surfaces that overlap. The asymmetrical drag force acting on these surfaces drives the turbine's rotation. Two half-circles make up the simplest Savonius turbine blade profile. Nonetheless, several academics have suggested altered blade designs that improve the Savonius Hydrokinetic Turbine's (SHT) performance [18], [19], [20].

Therefore, this study aims to evaluate the performance of a double-Savonius hydrokinetic turbine at varying TSR values through numerical simulation. The investigation focuses on the relationship between Cp, Cm, and flow contours to identify the optimal operating condition for maximum efficiency. The research contribution is the identification of the optimal TSR for a double-Savonius hydrokinetic turbine, supported by CFD-based analyses of power and moment coefficients and flow behavior, which provide new insights into the aerodynamic and hydrodynamic optimization of small-scale hydrokinetic systems.

## 2 Research methods

This research was conducted using a Computational Fluid Dynamics (CFD) approach using ANSYS Fluent 2023 software, which is widely used to solve various fluid problems, such as heat exchanger [21], [22], Combustion [23], [24], and other thermal and fluids problems [25], [26]. The simulation was run on a computer with an Intel Core i7 processor and 32 GB of RAM. The simulation process began with creating a turbine blade model and a flow domain in SpaceClaim, which were then integrated with ANSYS Fluent. A drawing of the turbine blade is shown in Fig. 1, while the blade dimensions and simulation domain are presented in Table 1.

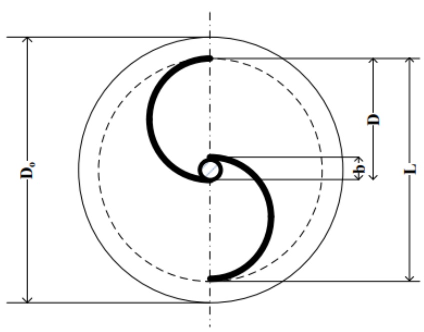

**Fig. 1.** Blade dimension.

**Table 1**. Blades parameter and value.

| Parameter | Value |
|---|---|
| Endplate Diameter ($D_0$) | 115 mm |
| Blade Diameter (D) | 60 mm |
| Savonius Diameter (L) | 110 mm |
| Turbine Axis Diameter (b) | 10 mm |
| Domain Length | 3400 mm |
| Domain Width | 500 mm |

After the design process is complete, the next step is meshing, which generates grids or discretized elements in the simulation domain. This process is critical because the quality of the mesh will affect the accuracy of the simulation results. Meshing was carried out using ANSYS Meshing, with a hexahedral mesh applied to the main area and a refinement around the turbine blades to capture velocity and pressure gradients more accurately. The mesh results from this study are shown in Fig. 2.

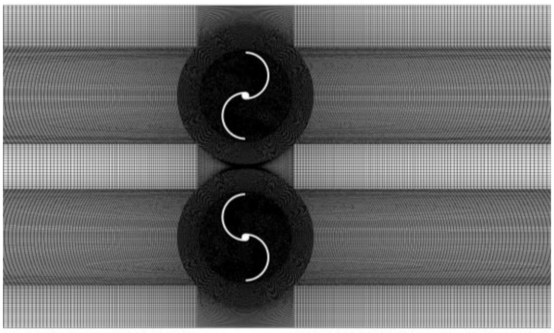

**Fig. 2.** Mesh for this simulation.

Once the meshing is complete, the next step is to name each part of the domain, such as the inlet, outlet, turbine wall, and domain wall. Naming facilitates the determination of boundary conditions and the precise setting of simulation parameters for each relevant part. In the simulation, several model choices and boundary condition parameters were specified. To dynamically capture time changes, we employed a pressure-based solver with transient time conditions. The K-Omega SST model, which performs well in flows with strong pressure gradients, is used to model viscosity. The K-Omega SST model, which combines two previous turbulence models, the k-ω (k-omega) model and the k-ε (k-epsilon) model, was typically employed for turbulence flow [27]. To improve momentum precision, the second-order upwind approach is used. The selected solver algorithm is a Coupled Solver, renowned for its high stability and accuracy in enforcing momentum conservation.

The boundary conditions used in this study are shown in Table 2. The determination of these boundary conditions is adjusted to the flow characteristics and configuration of the simulation domain.

**Table 2.** Boundary condition.

| Condition | Value |
|---|---|
| Velocity Inlet | 0.2 m/s |
| Turbulence Intensity | 0.5% |
| Turbulence Length Scale | 0.028 |
| Backflow Pressure outlet | 1 atm |

In this study, the Tip-Speed Ratio (TSR) value is entered for each turbine blade. TSR is an essential parameter in turbine performance analysis because it indicates the ratio of the blade tip speed to the fluid velocity that the blade experiences. The equation for calculating the Tip-Speed Ratio (TSR) for a turbine equipped with airfoil-shaped blades is as follows:

$$TSR = \frac{\omega R}{V} \tag{1}$$

Where:
ω = angular velocity (rad/s)
R = Blade radius (m)
V = Inlet velocity (m/s)

In this study, we varied the TSR from 0.2 to 2.0 in increments of 0.2. This variation was conducted to determine the effect of TSR changes on turbine performance, particularly on the resulting power coefficient and moment coefficient. The methodology flowchart is shown in Fig. 3.

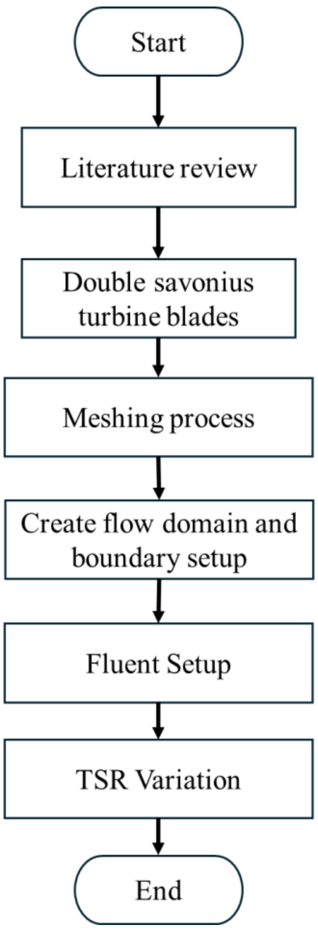


**Fig. 3.** Research flowchart.

## 3 Results and discussion

After conducting simulations for each Tip-Speed Ratio (TSR) value, the next step is to analyze the data by visualizing velocity contours. This visualization provides a deeper understanding of the fluid flow behavior around the turbine during operation. Velocity contours offer information on the direction and magnitude of fluid flow within the simulation domain. Through these contours, flow patterns around the turbine can be identified, including the emergence of critical phenomena such as recirculation zones, vortex formation, and flow separation from the blade surface.

The presence of these phenomena significantly impacts turbine efficiency and performance. Therefore, analysis of velocity contours not only helps understand the interaction between the fluid and the structure but also provides a crucial basis for evaluating and optimizing turbine designs to achieve better performance. Fig. 4. shows the pressure contour for TSR 0.2. At this TSR, the turbine blades rotate at a speed lower than the fluid velocity, resulting in the formation of vortices and a large recirculation region behind the turbine. This condition leads to significant energy losses due to suboptimal interaction between the blades and the fluid.

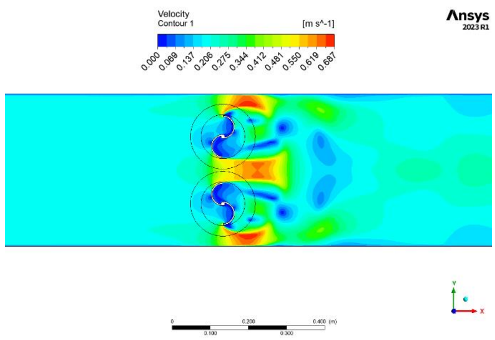


**Fig. 4.** Velocity contour for TSR 0.2.

At TSR 1.0, as shown in Fig. 5, based on the velocity contour results, there is a balance between the blade velocity and the fluid velocity, making this condition optimal for a hydrokinetic Savonius turbine. The flow distribution behind the turbine appears more symmetrical, the vortices are more controlled, and the overall flow pattern indicates improved efficiency.

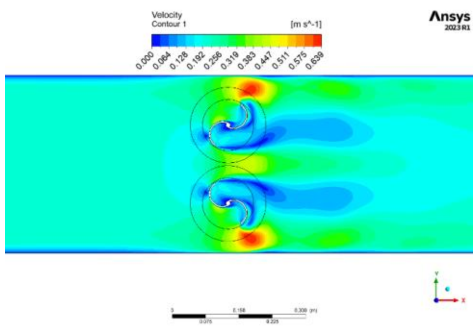


**Fig. 5.** Velocity contour for TSR 1.0.

At TSR 2.0, as shown in Fig. 6, the turbine blades rotate too quickly relative to the fluid velocity. As a result, the interaction between the fluid and the blades becomes less effective. The resulting vortices appear irregular, with a chaotic flow pattern and frequent flow separations. The fluid tends not to follow the blade contours properly, leading to reduced lift and increased drag.

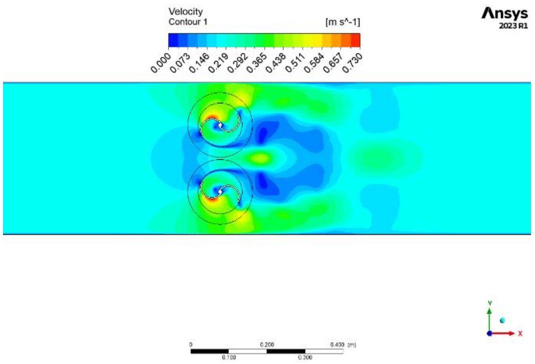


**Fig. 6.** Velocity contour for TSR 2.0.

After obtaining simulation results for each Tip-Speed Ratio (TSR) value, the next step is to calculate the power coefficient (Cp). The power coefficient is a key parameter that indicates how efficiently the turbine converts the kinetic energy of the fluid into mechanical energy. The Cp value is calculated from torque and angular velocity data generated by the simulation, along with the fluid velocity and density flowing through the turbine's swept area. Determining the average power coefficient of flowing water involves the following calculation.

$$C_p = \frac{P_{mechanical}}{P_{available}} = \frac{T.\omega}{0.5\rho A_f U^3} \quad (2)$$

Where the average torque of the enginer turbine is $T\ (Nm)$, the angle speed of the turbine is $\omega\ (rad/s)$, the water density is $\rho\ (kg/m^3)$, the rotary frontal area is $A_f\ (m^2)$, and the flow water speed is $U\ (m/s)$. where the speed at the rotor angle is $\omega\ (rad/s)$, the rotor area is $r\ (m)$, and the fluid flow speed is $U\ (m/s)$. These equations are fundamental to fluid flow and describe the water flow around the turbine. The continuity equation is a principle that ensures the mass of the fluid is conserved throughout the flow process.

Based on the calculations, the power coefficient (Cp) increased from a TSR of 0.2 to a peak of 1.0. After that, the Cp value decreased relatively to a TSR of 2.0. This pattern indicates that a TSR of 1.0 is the most efficient operating condition for the Savonius turbine in this study. This finding is in line with the results reported by Alizadeh et al. [19], which also showed that there is an optimum TSR value that produces maximum efficiency before decreasing at higher TSRs due to less effective fluid-blade interactions as shown in Fig 7.

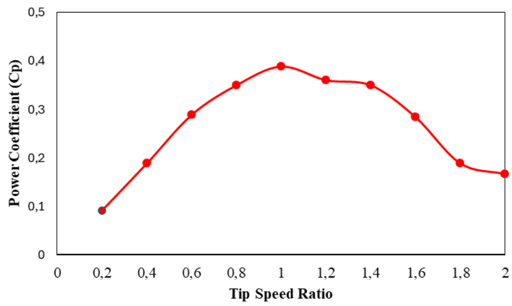


**Fig. 7.** Power coefficient.

The torque coefficient $C_t$ Can be calculated using the following equation:

$$C_m = \frac{C_p}{TSR} \quad (3)$$

In this equation, Cm represents the torque coefficient, Cp is the power coefficient, and TSR denotes the tip-speed ratio. Both Cm and Cp are critical parameters for evaluating the performance and efficiency of turbine designs. While Cp reflects how effectively the turbine converts the kinetic energy of the fluid into mechanical power, Cm provides insight into the rotational force (torque) generated by the turbine relative to the available dynamic pressure and the turbine's swept area.

Understanding the relationship between Cm and Cp across varying TSR values enables more accurate prediction of turbine behavior across a range of flow conditions. This is particularly important for optimizing blade geometry, rotational speed, and load matching in real-world applications, where both torque and power output are essential in determining the overall effectiveness of a hydrokinetic energy system.

Fig. 8 shows the variation in the moment coefficient (Cm) as a function of the Tip Speed Ratio (TSR). Based on the graph, Cm reaches a maximum value at a TSR of around 0.5. This indicates that under these conditions, the turbine produces maximum torque relative to the dynamic pressure and blade swept area.

After passing this peak, the Cm value tends to decrease as the TSR increases. This decrease indicates that the turbine produces less torque at high TSR, a common characteristic of drag-based turbines such as the Savonius. Excessively high rotational speeds decrease the pressure difference between the blades, increase flow separation, and promote wake interaction, thereby reducing torque generation efficiency.

The decreasing trend in Cm at high TSR indicates that the turbine is becoming less efficient at generating torque, even though the power coefficient (Cp) may still be moderate. Therefore, it is essential to operate the turbine within the optimal TSR range, which is around 0.4 to 0.6, to ensure effective energy conversion, especially under low or unstable flow conditions.

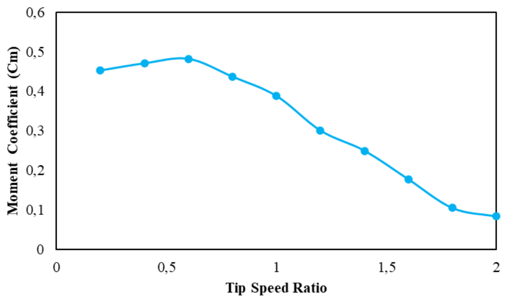


**Fig. 8.** Moment coefficient.

## 4 Conclusion

Simulation and calculation results indicate that the Savonius hydrokinetic turbine achieves its maximum power coefficient (Cp) at a Tip Speed Ratio (TSR) of 1.0, corresponding to the highest energy conversion efficiency. Analyses of velocity and pressure contours show stable and symmetrical flow distribution around the turbine blades, with well-formed vortices that generate maximum torque. The moment coefficient (Cm) attains its highest value at low TSR (0.4–0.5) and decreases as TSR increases, reaching a minimum at TSR = 2.0. These results demonstrate that TSR = 1.0 is the optimal operating point, balancing flow pattern and torque generation to maximize turbine efficiency. This study advances the understanding of fluid–structure interaction and flow dynamics in double-Savonius hydrokinetic turbines.

By integrating performance parameters (Cp and Cm) with contour-based flow visualization, it provides a comprehensive interpretation of the influence of TSR variations on turbine efficiency and flow stability. The integrated CFD-based framework strengthens the theoretical foundation for optimizing the performance of vertical-axis hydrokinetic turbines in low-velocity water flows. A primary limitation of this study is its reliance on a two-dimensional (2D) simulation approach, which does not fully capture three-dimensional flow phenomena such as tip vortices, secondary flows, and end-plate interactions.

Future research should prioritize three-dimensional CFD simulations and experimental validation to confirm and refine these numerical results. Further investigation into the effects of installing a barrier plate around the turbine may also yield valuable insights into flow-control strategies to improve power performance. In summary, this research offers practical and theoretical insights into the optimal operating characteristics of double-Savonius hydrokinetic turbines. The findings identify TSR = 1.0 as the most efficient operating point and lay the foundation for future studies on geometric optimization and experimental implementation in real water-flow environments.

## References

1. R. Selvaraj, V. M. Kuthadi, and S. Baskar, Smart building energy management and monitoring system based on artificial intelligence in smart city. Sustainable Energy Technologies and Assessments. **56** (2023). https://doi.org/10.1016/j.seta.2023.103090
2. D. L. Pamuttu, M. Akbar, A. P. Andika, and H. Hariyanto, An Investigation of Hybrid Renewable Energy Potential by Harnessing Traffic Flow. International Journal of Heat and Technology. **41**, 1 (2023). https://doi.org/10.18280/ijht.410126
3. Ç. Iris and J. S. L. Lam, Optimal energy management and operations planning in seaports with smart grid while harnessing renewable energy under uncertainty. Omega (United Kingdom). **103** (2021). https://doi.org/10.1016/j.omega.2021.102445
4. M. Dhalwala, A. Bayram, P. Oshkai, and A. Korobenko, Performance and near-wake analysis of a vertical-axis hydrokinetic turbine under a turbulent inflow. Ocean Engineering. **257** (2022). https://doi.org/10.1016/j.oceaneng.2022.111703
5. M. T. Tigabu, M. S. U. Khalid, D. Wood, and B. T. Admasu, Some effects of turbine inertia on the starting performance of vertical-axis hydrokinetic turbine. Ocean Engineering. **252** (2022). https://doi.org/10.1016/j.oceaneng.2022.111143
6. A. B. Mohamed, C. Bear, M. Bear, and A. Korobenko, Performance analysis of two vertical-axis hydrokinetic turbines using variational multiscale method. Comput Fluids. **200** (2020). https://doi.org/10.1016/j.compfluid.2020.104432
7. N. Guillaud, G. Balarac, E. Goncalvès, and J. Zanette. Large Eddy Simulations on Vertical Axis Hydrokinetic Turbines - Power coefficient analysis for various solidities. Renew Energy. **147** (2020). https://doi.org/10.1016/j.renene.2019.08.039
8. R. K. Chaulagain, L. Poudel, and S. Maharjan, A review on non-conventional hydropower turbines and their selection for ultra-low-head applications. Heliyon. **9**, 7 (2023)
9. A. K. Nag and S. Sarkar, Performance analysis of Helical Savonius Hydrokinetic turbines arranged in array. Ocean Engineering. **241** (2021)
10. M. Kulak, M. Lipian, K. Olasek, M. Pereira, and F. Ravelet, Rotor solidity and blade pitch influence on horizontal axis small wind turbine performance–Experimental study. Energy Reports. **12**, 4568–4577 (2024)
11. W. I. Ibrahim, M. R. Mohamed, and R. Ismail, Modelling of Power Curve Equation for Small-

Scale Vertical Axis Hydrokinetic Turbine. Proceedings of the 6th International Conference on Electrical, Control and Computer Engineering: InECCE2021, 57–67 (2022)
12. R. Kumar and A. Kumar, Influence of Design Parameters on the Performance of Slotted Savonius Hydrokinetic Turbine. Results in Engineering. 105768 (2025)
13. T. S. Rengma, M. K. Gupta, and P. M. V. Subbarao, A novel method of optimizing the Savonius hydrokinetic turbine blades using Bezier curve. Renew Energy. **216** (2023)
14. O. Doso and S. Gao, Application of savonius rotor for hydrokinetic power generation. Journal of Energy Resources Technology, Transactions of the ASME. **142**, 1 (2020). https://doi.org/10.1115/1.4044555
15. N. R. Maldar, C. Y. Ng, and E. Oguz, A review of the optimization studies for Savonius turbine considering hydrokinetic applications. Energy Convers Manag. **226**, (2020). https://doi.org/10.1016/j.enconman.2020.113495
16. R. A. Moniruzzaman, M. Chowdhury, M. S. H. Saha, D. Billah, M. M. Helal, and A. Biswash, Hydrokinetic Turbine Technology and Its Prospect in Bangladesh: A Review. Australian Journal of Engineering and Innovative Technology. (2022). https://doi.org/10.34104/ajeit.022.01007
17. M. Mohammed, S. Sarip, and W. A. Mustafa, Systematic Review of Computational Fluid Dynamics Modelling and Simulation Techniques Employed in Vertical Axis Hydrokinetic Turbines. Journal of Advanced Research in Applied Mechanics. **117**, 51–71 (2024)
18. I. Hashem and B. Zhu, Metamodeling-based parametric optimization of a bio-inspired Savonius-type hydrokinetic turbine. Renew Energy. **180**, 560–576 (2021)
19. H. Alizadeh, M. H. Jahangir, and R. Ghasempour, CFD-based improvement of Savonius type hydrokinetic turbine using optimized barrier at the low-speed flows. Ocean Engineering. **202**, (2020). https://doi.org/10.1016/j.oceaneng.2020.107178
20. C. M. Shashikumar, H. Vijaykumar, and M. Vasudeva, Numerical investigation of conventional and tapered Savonius hydrokinetic turbines for low-velocity hydropower application in an irrigation channel. Sustainable Energy Technologies and Assessments. **43** (2021)
21. G. Anjaneya, et al, Numerical simulation of microchannel heat exchanger using CFD. International Journal on Interactive Design and Manufacturing (IJIDeM). **18**, 5847–5863 (2024)
22. X. Y. Zhang, Y. T. Ge, and P. Y. Lang, Experimental investigation and CFD modelling analysis of finned-tube PCM heat exchanger for space heating. Appl Therm Eng. **244** (2024)
23. A. Purwanto, H. Saputro, A. F. Alhikami, and F. A. Munir, Enhancing Stoichiometric Methane-Air Flames: The Role of N2O Replacement. Automotive Experiences. **8**, 2, (2025
24. H. Saputro, L. Fitriana, A. Purwanto, F. A. Munir, and W.-C. Wang, A Development of Meso-Scale Vortex Combustion for a Micro Power Generator Based on a Thermoelectric Generator. Fluids. **7**, 386 (2022). https://www.mdpi.com/2311-5521/7/12/386
25. M. Szudarek and J. Piechna, CFD analysis of the influence of the front wing setup on a time attack sports car's aerodynamics. Energies (Basel). **14**, 7907 (2021)
26. J. M. Luckring and A. Rizzi, Prediction of concentrated vortex aerodynamics: Current CFD capability survey. Progress in Aerospace Sciences. **147** (2024)
27. ANSYS Inc, ANSYS Fluent Theory Guide Release 15. (2013)